Digital Suppression of Transmitter Leakage in FDD RF Transceivers with an Enhanced Low Sampling Rate Behavioral Model

Wenhui Cao, *Student Member, IEEE*, Yue Li, *Student Member, IEEE*, Guoqing Luo, Zhangcheng Hao, and Anding Zhu, *Senior Member, IEEE*

***Abstract*—With continuously increasing of signal bandwidth, the transmitter leakage issue in frequency division duplexer (FDD) transceivers becomes severer. In this letter, an enhanced behavioral model is proposed to suppress FDD transmitter leakage at a low-sampling rate. The theoretical analysis is provided to explain the operation principle of the proposed model. The experimental results show that the proposed model can effectively increase the accuracy of generating sideband replica and thus improve the suppression performance.**

***Index Terms*—frequency division duplexer, phase accuracy, phase-related nonlinearity, suppression model, TX leakage.**

I. Introduction

In frequency division duplexer (FDD) systems, the transceiver simultaneously transmit and receive signals using the same antenna, which can lead that the received signals are contaminated by the transmitting signal leakages, as shown in Fig. 1. The filter in duplexer can suppress the transmitter (TX) leakage to some extent, but the residual leakage can still affect the received signal if the leakage power is high. Digital suppression [1] [2] has been considered as an effective technique to mitigate TX leakages. It applies a digital model to regenerate the leakage replica and then subtracts it from the received signal.

Due to a nonlinear process involved, the sampling rate of the signal must be set high enough during the digital replica signal generation to avoid aliasing effect. In future systems, e.g., fifth generation (5G), the data rate and signal bandwidth will continue to increase. A direct consequence of the high sampling rate requirement is that the digital block of the behavioral model is required to work at a very high data rate, e.g., over giga-sample per second, that is not feasible in practice. To reduce the data processing rate, W. Cao et al. in [3] proposed an alternative algorithm based on decomposed vector rotation (DVR) model [4] to perform the sideband suppression at a low processing rate. The idea was to use cross-term products to eliminate the aliasing distortion in replica generation. However, to achieve a high accuracy, a large number of cross-term products are required, which can increase the model implementation complexity.

After theoretical analysis of magnitude- and phase- related nonlinearity generations, this letter proposes an enhanced model for sideband suppression. Comparing with the model in [3], the new model can achieve a higher accuracy in generating the sideband replica with a lower residual inference and using a smaller number of coefficients.

II. Theoretical Analysis

The block diagram of sideband suppression is shown in Fig. 1, where the baseband input signal $\tilde{x}(n)$ is fed into a sideband suppression block to produce the output spectral replica $\tilde{v}(n)$ that can be subtracted from the received signal to restore the fidelity of the received information. As described in [3], the digital signal processing of replica generation includes three parts: 1) frequency shift; 2) nonlinear modeling; 3) band-limited filtering. The frequency shift is carried out by multiplying $e^{j\Delta\omega n}$. A behavioral model, e.g., the DVR model [4], can be used to model the nonlinearity of the PA, and finally the corresponding sideband resplica falling in the receiver band can be extracted by using a band-limited FIR filter.

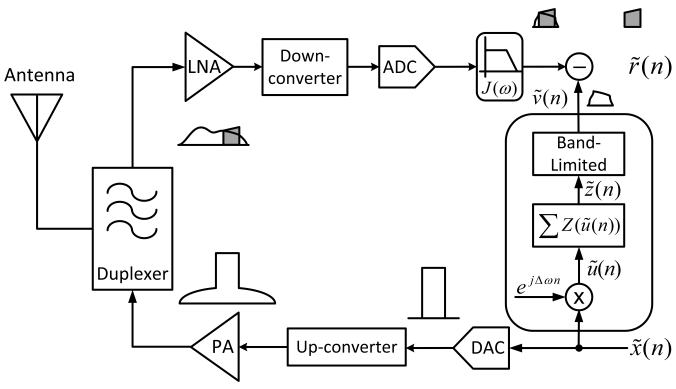

Fig. 1. TX leakage in FDD transceivers and the block diagram of sideband suppression at digital baseband.

Because of spectrum regrowth, the signal bandwidth is expanded after the nonlinear modeling. To avoid aliasing

This work was supported in part by Natural Science Foundation of China 61722107 and 61801152, in part by the State Key Laboratory of Millimeter Wave program K201909, and in part by Science Foundation Ireland under grant number 16/IA/4449. *(Corresponding author: Guoqing Luo)*

W. Cao is with the Key Lab of RF Circuits & System of Ministry of Education, Hangzhou Dianzi University, Hangzhou, and also with the State Key Lab of Millimeter Waves, Southeast University, Nanjing, China.

G. Luo is with the Key Lab of RF Circuits & System of Ministry of Education, Hangzhou Dianzi University, Hangzhou, China (E-mail: luoguoqing@hdu.edu.cn).

Z. Hao is with the State Key Lab of Millimeter Waves, Southeast University, Nanjing, China.

Y. Li and A. Zhu are with the School of Electrical and Electronic Engineering, University College Dublin, Dublin 4, Ireland.

effect, the input signal is usually required to be sampled at a high sampling rate, which can lead to high implementation complexity and high power consumption because the digital circuit must be operated at a high clock rate. In [3], we discovered that the aliasing effect can be compensated by using certain cross-terms in the behavioral model. This can be explained as follows.

For example, if the signal $\tilde{u}(n)$ is down-sampled by 2, to recover the lost information, the lost sample $\tilde{u}(2)$ can be approximated by the average of adjacent samples $\tilde{u}(1)$ and $\tilde{u}(3)$,

$$\tilde{u}(2) = [\tilde{u}(1) + \tilde{u}(3)]/2. \tag{1}$$

Substituting (1) into the 3rd-order polynomial of $\tilde{u}(2)$, we obtain that

$$\begin{aligned} &|\tilde{u}(2)|^2\tilde{u}(2) \\ &= \frac{[|\tilde{u}(1)|^2 + |\tilde{u}(3)|^2 + 2\,|\tilde{u}(1)|\,|\tilde{u}(3)|\cos(\theta_1 - \theta_3)] \times \tilde{u}(1)}{8} \\ &+ \frac{[|\tilde{u}(1)|^2 + |\tilde{u}(3)|^2 + 2\,|\tilde{u}(1)|\,|\tilde{u}(3)|\cos(\theta_1 - \theta_3)] \times \tilde{u}(3)}{8}. \end{aligned} \tag{2}$$

where θ_1, θ_3 are the phase information of samples $\tilde{u}(1)$, $\tilde{u}(3)$, respectively. From (2), we can see that the 3rd-order polynomial term of $\tilde{u}(2)$ can be approximated by using combination products of $\tilde{u}(1)$ and $\tilde{u}(3)$, e.g., cross-term products $|\tilde{u}(1)|^2\tilde{u}(3)$, $|\tilde{u}(3)|^2\tilde{u}(1)$, $|\tilde{u}(1)||\tilde{u}(3)|\tilde{u}(3)$, and $|\tilde{u}(1)||\tilde{u}(3)|\tilde{u}(1)$. In [3], we have shown that these cross-terms can be implemented by using specific nonlinear operator in DVR model, e.g., $||\tilde{u}(n-i)| - \beta_k|\tilde{u}(n)|$, where β_k is the threshold value. Experimental results showed that, by using this approach, the aliasing effect can be compensated and therefore the suppression model can be operated at a low sampling rate. To achieve high accuracy, however, a large number of cross-term products are required, which can increase the model implementation complexity.

A. Phase Approximation Issue

If we carefully investigate (2), we can see that the DVR cross terms, $||\tilde{u}(n-i)| - \beta_k|\tilde{u}(n)|$, are only able to approximate the magnitude-related nonlinearity. The phase-related element, i.e., $cos(\theta_n - \theta_{n+i}) = cos(\Delta\theta_n)$, is omitted. It is ok when the sampling rate is reasonably high where $cos(\Delta\theta_n)$ can be approximated by a constant. However, under a severely reduced sampling rate, the value of the phase element $cos(\Delta\theta_n)$ can change significantly because the phase variations between two adjacent samples can be large. In Fig. 2 (a), the experimental results illustrate the distributions of $cos(\Delta\theta_n)$ at different sampling rates. What we found is that when the sampling rate is 368.64 MHz, around 90% of $cos(\Delta\theta)$ is in the range of [0.98, 1]. However, after reducing the sampling rate, the probability of $cos(\Delta\theta)$ in [0.98, 1] drops quickly, e.g., moving to the ranges of [0.85,0.98), [0.5,0.85), [0,0.5). In Fig. 2 (b), we can see that $cos(\Delta\theta)$ distribution is spread in a wider range at 61.44 MHz. This indicates that the approximation accuracy using the DVR nonlinear operators may be degraded if the variations of the phase element are not considered.

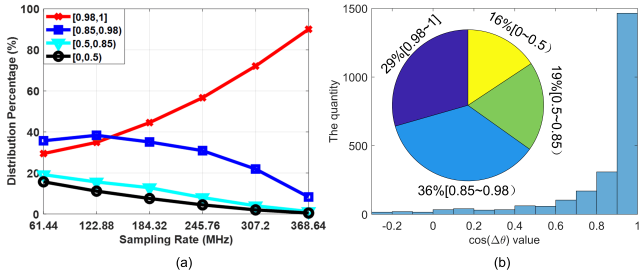

Fig. 2. (a) The distribution ranges of $cos(\Delta\theta)$ values with respect to different sampling rates and (b) the distribution of $cos(\Delta\theta)$ values at 61.44 MHz.

B. The Proposed Model

To accurately restore the missing digital samples and their corresponding high-order nonlinearities, both magnitude and phase approximations must be taken into account. After a thorough investigation and considering the special characteristics of the DVR model, we find that, the phase variation can be included in the model approximation by directly inserting the cross-term summation $[\tilde{u}(n-i) + \tilde{u}(n-i+1)]$ into the DVR operator, namely, using $||\tilde{u}(n-i) + \tilde{u}(n-i+1)| - \beta_k|\tilde{u}(n)|$, instead of $||\tilde{u}(n-i)| - \beta_k|\tilde{u}(n)|$. Because the summation of $[\tilde{u}(n-i)+\tilde{u}(n-i+1)]$ includes phase variations between two adjacent samples, the model accuracy now can be improved.

The direct summation of $[\tilde{u}(n-i) + \tilde{u}(n-i+1)]$ puts the same weight on the adjacent samples. In practical applications, the PA nonlinearity may be affected differently by the different samples. To flexibly adjust the weighting ratio, we introduce a parameter λ into the cross-term summation and obtain $[\tilde{u}(n-i) + \lambda\tilde{u}(n-i+1)]$. The final suppression model is expressed as

$$\begin{aligned} \tilde{z}(n) &= \sum_{i=0}^{M} \tilde{c}_{i,0}\tilde{u}(n-i) \\ &+ \sum_{k=1}^{K}\sum_{i=0}^{M}\{\tilde{c}_{ki,1}||\tilde{u}(n-i) + \lambda\tilde{u}(n-i+1)| - (1+\lambda)\beta_k| \\ &\quad \cdot e^{j\theta(n-i)}\} \\ &+ \sum_{k=1}^{K}\sum_{i=0}^{M}\{\tilde{c}_{ki,21}||\tilde{u}(n-i) + \lambda\tilde{u}(n-i+1)| - (1+\lambda)\beta_k| \\ &\quad \cdot e^{j\theta(n-i)} \cdot |\tilde{u}(n)|\} \\ &+ \cdots \end{aligned} \tag{3}$$

where the inner $|\cdot|$ returns the magnitude of input, while the outer $|\cdot|$ denotes the absolute value operation. To maintain linear in parameter, we can set λ to a fixed value and use linear optimization algorithms to extract the initial model coefficients. Later a $\pm\Delta\lambda$ perturbation or parameter sweep can be carried out to search the optimal coefficients.

III. Experimental Results

To verify the proposed model, a PA test platform was set up, as described in [3]. In the TX chain, the baseband signal in in-phase and quadrature form was modulated, up-converted to RF frequency, and amplified by the PA. In the receiver

(RX) chain, PA output was sampled and sent to a PC. The time alignment and model extraction were operated off-line in MATLAB.

For a fair comparison, all the experimental conditions were set the same as that in [3]. An in-house designed LDMOS PA was operated at 2.14 GHz and excited by a 20-MHz input signal with 6.5 dB PAPR. The PA output spectrum was captured at a high sampling rate of 368.64 MSPS, from which a 20-MHz sideband was filtered as TX leakage. The TX-RX frequency gap was 30.72MHz. The residual interference was obtained by subtracting the sideband replica from TX leakage interference. For comparison, the TX leakage suppression at a full speed is shown in Fig. 3 (a). After down-sampling from 368.64 MHz to 61.44 MHz, a strong aliasing interference is shown in Fig. 3 (b).

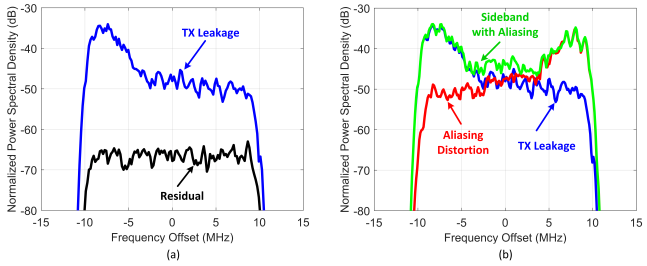

Fig. 3. (a) The full-band performance reference and (b) the spectral demonstration with aliasing effect.

In the low-sampling rate scenario, the proposed model was compared against the DVR model. The DVR model applies 83 coefficients, M=3, K=10. On the contrary, with M=4 and K=5, the proposed model deploys 59 coefficients. To determine λ value, the parameter sweep method has been conducted. The Normalized Mean Squared Error (NMSE) value of sideband replica with respect to λ value is depicted in Fig. 4 (a). It indicates that when λ=6.3, the proposed model can achieve an optimal sideband estimation. In low sampling rate scenario, the performance comparisons of DVR and proposed models are illustrated in Fig. 4 (b) and Table I. It reports that the proposed model can improve the suppression performance with a smaller number of coefficients. Moreover, it shows that with λ=1.0, satisfactory results can be achieved. In applications with less stringent requirements, λ could be preset as 1.0 to reduce the complexity of model extraction.

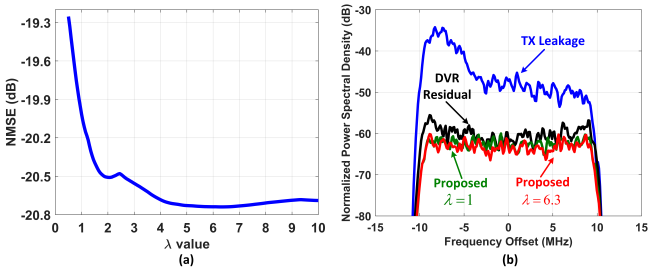

Fig. 4. (a) The relationship between λ and NMSE and (b) the suppression comparisons between the DVR model and the proposed model.

TABLE I
COMPARISONS BETWEEN DVR AND THE PROPOSED MODEL

	No. of Coeff.	NMSE (dB)	Residual Interference (dB)
DVR model	83	-17.48	-60
Proposed Model	59 ($\lambda = 6.3$)	-20.73	-62.3
	59 ($\lambda = 1.0$)	-20.02	-61.5

More experiments were carried out to verify the proposed model in different sampling rates. The full-band sampling rate was down sampled to 92.16 MHz, 73.73 MHz and 61.44 MHz, respectively. The results in Fig. 5 (a) show that λ value affects the accuracy more at lower sampling rates. This is because phase variations appear more significant at a lower sampling rate. Furthermore, at sampling rate of 61.44 MHz, the curves of NMSE against λ with different receiver bandwidths are shown in Fig. 5 (b). All the curves exhibit the similar trends, which confirms the effectiveness and stability of the proposed model.

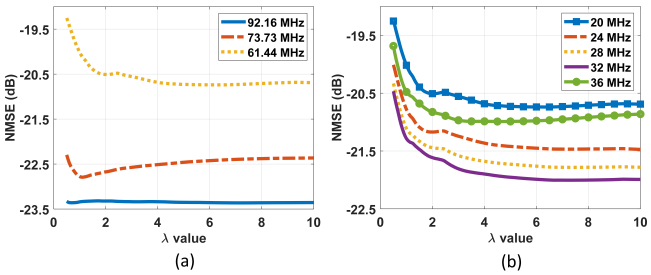

Fig. 5. (a) The relationship of NMSE vs. λ at different sampling rates and (b) NMSE vs. λ with different receiver bandwidths.

IV. CONCLUSION

An enhanced sideband suppression model has been introduced. The experimental results showed that the proposed model can effectively improve the sideband suppression performance with a smaller number of model coefficients. It can be a promising technique to be deployed in wideband 5G communication systems.

REFERENCES

[1] S. Farsi, H. Gheidi, H. T. Dabag, P. S. Gudem, D. Schreurs, and P. M. Asbeck, "Modeling of deterministic output emissions of power amplifiers into adjacent receive bands," *IEEE Trans. Microw. Theory Tech.*, vol. 63, no. 4, pp. 1250–1262, Apr. 2015.

[2] M. Omer, R. Rimini, P. Heidmann, and J. S. Kenney, "A compensation scheme to allow full duplex operation in the presence of highly nonlinear microwave components for 4G systems," in *IEEE MTT-S International Microwave Symposium Digest*, Jun. 2011, pp. 1–4.

[3] W. Cao, Y. Li, and A. Zhu, "Digital suppression of transmitter leakage in fdd rf transceivers: Aliasing elimination and model selection," *IEEE Transactions on Microwave Theory and Techniques*, vol. 66, no. 3, pp. 1500–1511, Mar. 2018.

[4] A. Zhu, "Decomposed vector rotation-based behavioral modeling for digital predistortion of RF power amplifiers," *IEEE Trans. Microw. Theory Tech.*, vol. 63, no. 2, pp. 737–744, Feb. 2015.